

# Median–Radial Function: A Robust, Covariance-Free Framework and Applications

Elsayed A. H. Elamir

Department of Management and Marketing, College of Business Administration, Kingdom of Bahrain

Email: [shabib@uob.edu.bh](mailto:shabib@uob.edu.bh)

## Abstract

A median-radius framework for assessing centrality in multivariate data using median distances is proposed. Based on the proposed framework, scale-invariant measure of radial dispersion is defined and used to establish a depth function that is robust to outliers and independent of covariance structure. The depth function does not depend on moment assumptions and naturally adapts to skewness, multimodality, and heavy-tailed distributions which make it effective for high dimension data structure. We demonstrate fundamental characteristics of the underlying functionals such as subgradient and convexity. The subgradients provide additional insight and encodes the imbalance in directional contributions of the data. This suggests a new approach to detect skewness and structural asymmetry through a purely radial construction. Empirical studies demonstrate that the method agrees with classical approaches under symmetry while providing a more flexible and informative characterization in complex settings.

**Keywords:** geometric centrality; high-dimensional data; MAD; multivariate analysis; robust estimation; statistical depth.

Subject classification code: 62G30 and 62G32

ORCID: 0000-0002-9430-072X

**Conflict of interest:** The author does not have any conflict of interest.

**Financial support:** This research did not receive any specific grant from funding agencies in the public, commercial, or not-for-profit sectors.

**AI Tool:** ChatGPT and copilot are used for improving language, readability and presentation

# 1 Introduction

Measures of multivariate centrality are traditionally based on either distance or depth. Classical distance-based methods are dominated by the Mahalanobis distance (“Reprint of: Mahalanobis, P.C. (1936) ‘On the Generalised Distance in Statistics.’” 2018) which incorporates covariance structure and yields affine-invariant elliptical geometry. While optimal under Gaussian assumptions, it is highly sensitive to outliers and becomes unreliable in high-dimensional settings due to instability of covariance estimation ((Rousseeuw & Driessen, 1999). While these methods are optimal under Gaussian assumptions, they are highly sensitive to outliers, heavy-tailed or skewed distributions, and become unstable in high-dimensional settings (Zuo & Serfling, 2000).

To improve robustness, a variety of affine-equivariant estimators of scatter have been proposed, including the minimum covariance determinant (MCD) and S-estimators (Rousseeuw & Croux, 1993). These lead to robust Mahalanobis distances with high breakdown points. These methods remain linked to covariance-based geometry and face significant challenges in high-dimensional settings. In this way the reliable estimation of scatter becomes difficult or impossible when  $d$  is comparable to or larger than  $n$  (Deb & Sen, 2023; Pawar & Shirke, 2022). To overcome these limitations, the concept of statistical depth was introduced to provide a centre-outward ordering of multivariate data without relying on moment assumptions (Tukey, 1975). A variety of depth functions have since been improved. Among the most influential depth notions are Tukey (halfspace) depth, This method measures the smallest probability mass over all halfspaces containing a point (Nagy, 2025; Zuo & Serfling, 2000). Simplicial depth used the probability that a point lies inside random simplices (Liu, 1990). Spatial depth uses expected directional vectors and provides a smooth notion of centrality (Chaudhuri, 1996). Projection depth depends on the worst standardized deviation over projection directions (Lange et al., 2014; Mosler & Mozharovskiy, 2022; Zuo, 2003).

These methods offer powerful geometric insights, but they often rely on directional projections, combinatorial constructions or moment-based normalization. This may limit their interpretability or computational efficiency in complex or high-dimensional settings. Therefore, median-based statistics play important role and well known for their robustness properties. The median absolute deviation (MAD) is a classic example of a high-breakdown scale estimator (Boente & Salibián-Barrera, 2021; Capezza et al., 2024; Lin & Chen, 2006; Rousseeuw & Croux, 1993) and its extension idea to multivariate settings, the geometric median.

Building on this, we generalize the median absolute deviation (MAD,  $\text{Med}|X - M|$ ,  $M$  median) by allowing the centre to vary for each fixed  $v$  ( $G(v) = \text{Med}|X - v|$ ). We call  $G(v)$  median-radius functional (MRF) or moving MAD.  $G(v)$  is the median radius needed to cover half of the data around  $v$ . Moreover, the associated normalized function  $H(v) = G(v)/\text{MAD}$  is defined. It serves as a scale-invariant measure of radial dispersion that quantifying how the median radius of the data cloud expands as the reference point moves away from the central location. In turn, inverse of  $H(v)$  provides a natural and interpretable depth measure where centrality is determined by the efficiency with which a point captures the bulk of the data.

This paper is organized as follows. Median-radius function is introduced in Section 2. The extension to multivariate setting is presented in Section 3. Introducing median-radial distance, median-radial depth and comparison with Mahalanobis distance are investigated in Section 4. Section 5 is devoted to conclusion.

## 2 Median-radius function

The median-radius function (MRF) or moving median absolute deviation (MMAD) is defined for any  $v \in \mathbb{R}$  by

$$G_X(v) = \text{Med}|X - v|.$$

It provides a robust, median-based measure of the dispersion of  $X$  around the reference point  $v$  rather than expected value (Elamir, 2025). It generalizes the classical MAD by allowing the centre to vary across the real line.

**Definition 1.** (Quantile representation of  $G(v)$ )

Let  $X$  be a real-valued random variable with cumulative distribution function  $F$ . For any  $v \in \mathbb{R}$  and  $r \geq 0$ , define the centred probability mass function

$$S_X(v, r) := \mathbb{P}(|X - v| \leq r) = F(v + r) - F(v - r).$$

The median–distance functional

$$G(v) = \text{Med}(|X - v|),$$

admits the quantile representation

$$G_X(v) = \inf \left\{ r \geq 0 : S_X(v, r) \geq \frac{1}{2} \right\}.$$

Thus  $G(v)$  is the smallest radius of symmetric interval  $[v - t, v + t]$  that captures probability at least  $1/2$ . In particular, the differentiability and smoothness properties of  $G(v)$  are governed by how the distribution allocates probability mass in arbitrarily small neighbourhoods of the boundary points  $v \pm G(v)$ . The following basic properties holds:

- 1)  $G(v)$  is convex in  $v \in \mathbb{R}$ : convexity of  $G(v)$  follows directly from convexity of absolute value combined with the monotonicity of the median operator (median preserves ordering).
- 2) Characterization via distribution function:  $G(v) \geq 0$  satisfies

$$F(v + G(v)) - F(v - G(v)) \geq \frac{1}{2}.$$

If the distribution of  $|X - v|$  has a unique median, then  $G(v)$  is the unique nonnegative solution of

$$F(v + G(v)) - F(v - G(v)) = \frac{1}{2}.$$

- 3) Value at a median: If  $M$  is a median of  $X$ , then:  $G(M) = \text{Med}(|X - M|)$ , which coincides with the population median absolute deviation (MAD) about the median.
- 4) Minimizers and relation to medians: Any median  $M$  of  $X$  minimizes  $G$ , i.e.  $G(v) \geq G(M)$ ,  $\forall v \in \mathbb{R}$ , with equality only at medians when the median is unique.
- 5) Lipschitz property: For all  $v, w \in \mathbb{R}$ ,  $|G(v) - G(w)| \leq |v - w|$ . In particular,  $G$  is 1-Lipschitz.

see, (Boyd & Vandenberghe, 2004).

**Definition 2** (Standardized  $G(v)$ )

Let  $X$  be a real-valued random variable with continuous distribution function  $F$ . Define

$$G(v) = \text{Med}(|X - v|), v \in \mathbb{R},$$

and let  $M$  denotes a median of  $X$ . The standardized MMAD is defined by

$$H(v) = \frac{G(v)}{G(\mu)} = \frac{\text{Med}(|X - v|)}{\text{Med}(|X - \mu|)}.$$

Thus,  $H(v)$  measures the median absolute deviation from  $v$ , normalized by its minimum value at the center ( $\mu$ ).

From properties of  $G(v)$ , the function  $H(v)$  has the following core properties:

- 1) Normalization and centrality:  $H(\mu) = 1, H(v) \geq 1 \quad \forall v$ , with equality if and only if  $v$  is a median (when unique). Therefore,  $H(v)$  quantifies relative dispersion from centre.
- 2) Convexity and shape: Since  $G(v)$  is convex,  $H(v)$  is convex. Consequently,  $H$  has a global minimum at  $M$ , no local minima other than the global one.
- 3) Lipschitz continuity: From the 1-Lipschitz property of  $G$ ,  $H$  is Lipschitz with constant  $1/G(M)$ .

The function  $H(v)$  is a normalized version of the median–radius functional  $G(v)$ , preserving its geometric and differential structure while providing a scale-free measure of centrality relative to the median.

**Definition 3.** (One-sided derivatives of  $G(v)$ )

Let  $X$  be a real-valued random variable with continuous distribution function  $F$ , and let

$$G(v) = \text{Med}|X - v|, \quad v \in \mathbb{R},$$

For any convex function, a fundamental subgradient result is

$$\partial G(v) = [G'_-(v), G'_+(v)].$$

where the left and right derivatives of  $G$  are defined by

$$G'_-(v) = \lim_{h \uparrow 0} \frac{G(v+h) - G(v)}{h}, \quad G'_+(v) = \lim_{h \downarrow 0} \frac{G(v+h) - G(v)}{h},$$

whenever these limits exist (Hubbard, 2015).

**Theorem 1.** Assume that the distribution function  $F$  of  $X$  is continuous. Define

$$G(v) = \text{Med}|X - v|.$$

Then the one-sided derivatives of  $G$  exist for every  $v \in \mathbb{R}$  and satisfy

$$\begin{aligned} G'_-(v) &= \mathbb{P}(X > v + G(v)) - \mathbb{P}(X \leq v - G(v)), \\ G'_+(v) &= \mathbb{P}(X \geq v - G(v)) - \mathbb{P}(X < v + G(v)). \end{aligned}$$

Moreover,  $G'_-(v), G'_+(v) \in [-1, 1]$ ,  $G'_-(v) \leq G'_+(v)$ , and  $0 \in [G'_-(v), G'_+(v)]$ . Therefore,  $v$  is a median of  $X$ .

*Proof.* see Appendix

The formulas show that the local slope of  $G(v)$  is determined entirely by the imbalance of probability mass outside the median-radius interval  $[v - G(v), v + G(v)]$ . In particular negative slope means more mass lies to the right, positive slope means more mass lies to the left and slope zero means perfect balance, i.e.  $v$  is a median.

**Corollary 1.** Under the assumptions of Theorem 1, the curvature of  $G$  at  $v$  can be obtained as

$$A(v) = G'_+(v) - G'_-(v).$$

Then

$$A(v) = \mathbb{P}(X = v - G(v)) + \mathbb{P}(X = v + G(v)).$$

In particular  $A(v) \geq 0$  for all  $v$ ,  $A(v) = 0$  if and only if  $G$  is differentiable at  $v$  and  $A(v) > 0$  if and only if the distribution of  $X$  places positive mass at one or both boundary points  $v \pm G(v)$ .

*Proof.* see Appendix

The corollary shows that curvature arises exactly when probability mass lies on the median-radius boundary. Thus, smooth regions of  $G$  correspond to continuously distributed mass away from the boundary while sharp corners of  $G$  correspond to bulk hitting the boundary and flat regions signal competing structure or multimodality. Note that, the interval  $[G'_-(v), G'_+(v)]$  coincides with the subdifferential  $\partial G(v)$  of the convex function  $G$  at  $v$ . Thus, the condition  $0 \in \partial G(v)$  characterizes precisely the set of minimizers of  $G$ , which is the median set of  $X$ .

Figure 1 is constructed using deterministic design points defined by the inverse normal distribution  $x = \Phi^{-1}(p)$ . This setting provides a noise-free approximation of the population-level behavior of  $G(v)$ . The resulting curves are smooth and perfectly symmetric, with a unique minimum at the center. The derivative exhibits a continuous transition across zero, and the absence of slope discontinuities (spike almost 0) confirms that, under a smooth continuous distribution, the median-radius functional is differentiable. This illustrates the intrinsic geometric structure of  $G(v)$  and  $H(v)$  in the absence of sampling variability. Note that the derivatives show symmetric left and right sides (symmetric distribution).

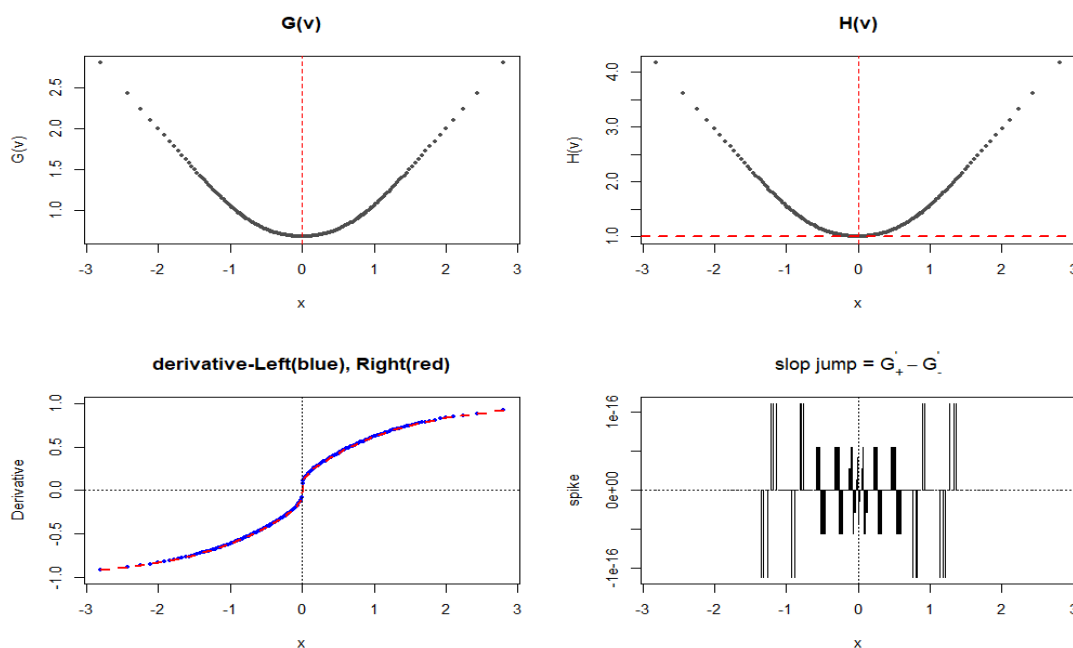


Figure 1. behaviour of  $G(v)$ ,  $H(v)$  and sub-gradient for a Gaussian  $N(0,1)$ .

Figure 2 shows the behaviour of the median-radius functional  $G(v)$  and its normalized version  $H(v)$ . Their derivatives are evaluated on a deterministic grid of size 200 using a mixture of three Gaussian quantile functions

$$x = (\Phi^{-1}(p; -2,0.75), \Phi^{-1}(p; 0,0.75), \Phi^{-1}(p; 3,0.8)),$$

where  $\Phi^{-1}(p; \mu, \sigma)$  denotes the inverse normal distribution with mean  $\mu$  and standard deviation  $\sigma$ .

This design produces a noise-free multimodal distribution consisting of three distinct values centred near  $-2$ ,  $0$ , and  $3$ . This allows a direct visualization of the population-level behavior of the functional without sampling variability. Unlike the unimodal case,  $G(v)$  exhibits a non-quadratic shape with multiple curvature regimes that indicates the presence of distinct clusters. The derivative plot reveals smooth but asymmetric transitions. This transition corresponds to regions where different components of the mixture dominate the median distance. The near-zero slope jumps indicate that the functional remains continuous but undergoes frequent local structural changes. This demonstrates that  $G(v)$  captures the underlying multimodal geometry through its level sets and differential properties.

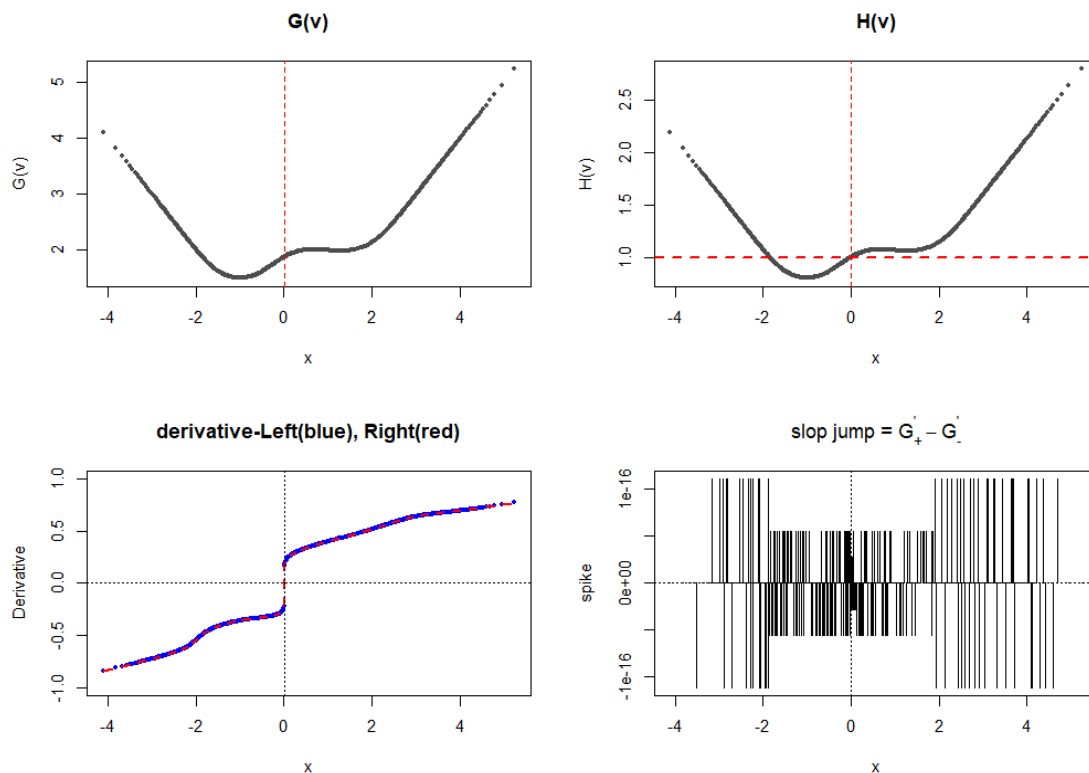


Figure 2. behaviour of  $G(v)$ ,  $H(v)$  and subgradient for a trimodal Gaussian mixture  $N(-2, 0.75^2)$ ,  $N(0, 0.75^2)$ , and  $N(3, 0.8^2)$ .

Figure 3 displays the behaviour of the median-radius functional  $G(v)$  and  $H(v)$ . The corresponding derivative diagnostics for a contaminated sample are defined as

$$x = (X_1, \dots, X_n), X_i \sim N(-3, 0.5), \text{ with 5 additional points from } N(3, 0.5).$$

This design represents a heavily skewed and contaminated distribution. The most observations are concentrated around  $-3$  while a small bulk of extreme points appears near  $+3$ . The purpose of this construction is to assess the robustness of the functional under severe imbalance and outliers. Despite the presence of a secondary cluster of outliers. The function  $G(v)$  retains a stable minimum determined solely by the main mass of data. The derivative structure further confirms that local behaviour is governed by the dominant cluster while the outlying observations exert negligible influence. Note that the derivatives show asymmetric right distribution where right side is longer than left side.

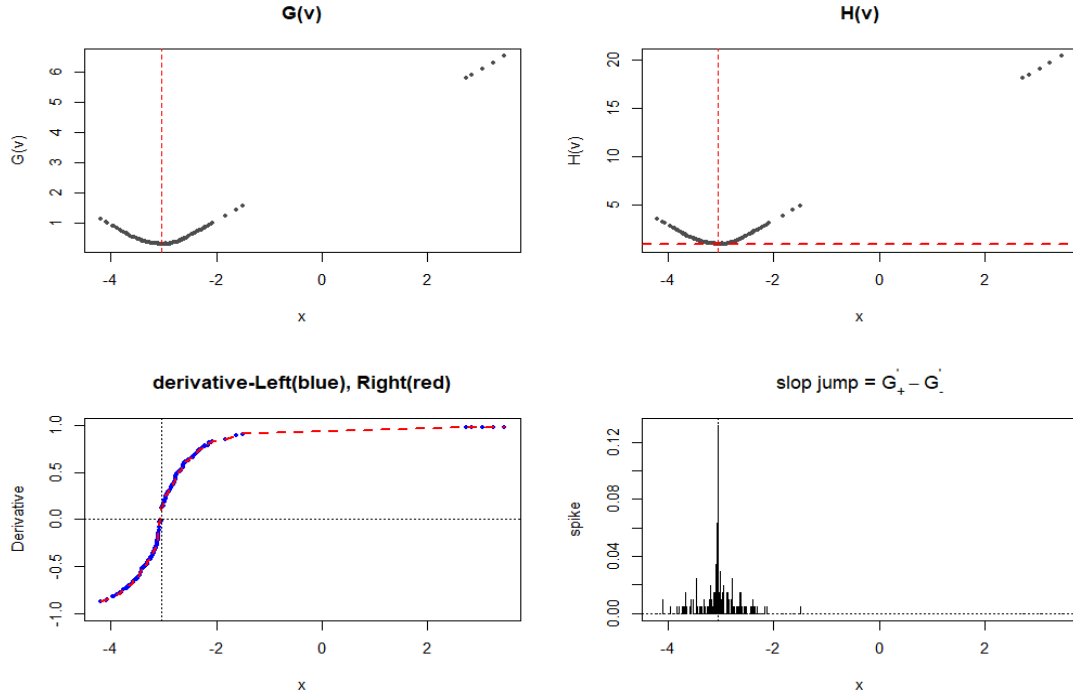


Figure 3. behaviour of  $G(v)$ ,  $H(v)$  and subgradient for contaminated Gaussian mixture  $N(-3, 0.5^2)$ , and  $N(3, 0.5^2)$ .

### 3 Multivariate Median-radius function

Let  $X$  be a random vector in  $\mathbb{R}^d$  with distribution  $F$ . The univariate function

$$G(v) = \text{Med}(|X - v|)$$

admits a natural and geometrically meaningful extension to the multivariate setting by replacing the absolute value with a norm. Throughout,  $\|\cdot\|$  denotes the Euclidean norm unless otherwise specified.

**Definition 4.** (Multivariate median–distance functional).

For any  $v \in \mathbb{R}^d$ , define

$$G(v) = \text{Med}(\|X - v\|),$$

the median of the distribution of the random variable  $\|X - v\|$ . Equivalently,  $G(v)$  is the smallest radius  $r \geq 0$  such that the closed Euclidean ball  $B(v, r)$  contains at least one half of the probability mass of  $F$

$$G(v) = \inf \left\{ r \geq 0: F(B(v, r)) \geq \frac{1}{2} \right\}.$$

Thus  $G(v)$  represents the median radius of the data cloud when viewed from the point  $v$ . The geometric median of  $X$  is defined as

$$M \in \arg \min_{v \in \mathbb{R}^d} \mathbb{E} \|X - v\|.$$

Under mild regularity conditions (e.g.,  $F$  not supported on a hyperplane), the geometric median exists and is unique. The corresponding central median–distance scale is

$$G(M) = \text{Med}(\|X - M\|),$$

which generalizes the univariate median absolute deviation (MAD) to the multivariate setting (Johnson R. & Wichern D., 2002).

**Definition 5.** (Standardized  $G(v)$ ).

The standardized version of  $G(v)$  is defined by

$$H(v) = \frac{\text{Med}(\|X - v\|)}{\text{Med}(\|X - m\|)} = \frac{G(v)}{G(m)}$$

by construction,

$$H(M) = 1, H(v) \geq 1 \text{ for all } v \in \mathbb{R}^d,$$

with equality if and only if  $v = M$ . Thus  $H(v)$  quantifies the relative inflation of the median radius when the centre is moved from the geometric median to a general point  $v$ .

The multivariate extensions  $G(v)$  and  $H(v)$  preserve the essential structural features of their univariate counterparts.

The  $G(v)$  and  $H(v)$  have the following core properties:

- 1) Convexity: the convexity of  $G(v)$  pursues from Euclidean distance convexity and the monotonicity of the median operator.  $H(v)$  is convex since it is a positive scaling of  $G(v)$ . Convexity ensures that the level sets

$$\{v \in \mathbb{R}^d : H(v) \leq c\},$$

are convex and nested. The level sets is a robust analogue of elliptical contours.

- 2) Orthogonal invariance: For any orthogonal matrix  $Q \in \mathbb{R}^{d \times d}$  and any vector  $b \in \mathbb{R}^d$ ,

$$G_{QX+b}(Qv + b) = G_X(v), H_{QX+b}(Qv + b) = H_X(v).$$

Thus  $G$  and  $H$  are invariant under rotations, reflections, and translations. This property follows from the invariance of the Euclidean norm under orthogonal transformations.

- 3) Robustness: since the geometric median  $M$  and the median distance  $G(M)$  possess a breakdown point of 50%. Therefore,  $H(v)$  inherits this robustness and remains stable under severe contamination or heavy-tailed distributions.

## 4 Applications

We investigate two applications of the median–radius framework. The standardized median–radial distance  $H(v)$  and the associated median–radius depth function  $D_{\text{MRD}}(v)$ . These constructions yield a unified geometry-driven approach to measure relative distance and statistical depth based solely on median radial behaviour.

### 4.1 Standardized median–radial distance

The standardized median–radial distance is defined by

$$H(v) = \frac{\text{Med}(\|X - v\|)}{\text{Med}(\|X - M\|)},$$

where  $M$  denotes the geometric median of  $X$ .

This functional is covariance-free, depending on Euclidean distances and invariant under orthogonal transformations. Since the geometric median and the median of distances are maximally robust estimators it possesses a high breakdown point of 50%. The function  $H(v)$  is convex in  $v$  and its level sets

$$\{v : H(v) = c\},$$

gives a natural geometric representation of centrality. As a scale-free quantity,  $H(v)$  exists for general distributions including heavy-tailed and infinite-variance cases. Importantly,  $H(v)$  adapts to the underlying data structure where it responds to skewness, multimodality, cluster separation, anisotropic tail behaviour and local density variations.

## 4.2 Comparison with Mahalanobis distance

We give a comparison with the classical and robust Mahalanobis distances. Focusing on their underlying assumptions, robustness properties, geometric behaviour and suitability for high-dimensional or heavy-tailed data. The classical Mahalanobis distance is defined as

$$D_M(v) = \sqrt{(v - \mu)^\top \Sigma^{-1} (v - \mu)},$$

$\mu$  and  $\Sigma$  denote the mean vector and covariance matrix of  $X$ , respectively.  $D_M(v)$  are affine invariance, elliptical geometry, and optimality under Gaussian assumptions. However, the Mahalanobis distance is not robust where  $\mu$  and  $\Sigma$  have breakdown point zero (Rousseeuw & Driessen, 1999). In addition, the method depends critically on the invertibility of  $\Sigma$  which restricts its applicability in modern high-dimensional settings where  $d$  may be comparable to or exceed  $n$ .

To overcome these issues, robust affine-equivariant estimators of location and scatter such as the minimum covariance determinant (MCD), S-estimators, and the orthogonalized Gnanadesikan–Kettenring (OGK) estimator are commonly used (Hubert et al., 2005). The resulting robust Mahalanobis distance is defined as

$$D_R(v) = \sqrt{(v - \hat{\mu})^\top \hat{\Sigma}^{-1} (v - \hat{\mu})}.$$

These methods improve robustness substantially with breakdown points approaching 50% depending on the choice of estimator. Despite these improvements,  $D_R(v)$  remains subject to several structural issues. First, they continue to rely on scatter estimation which can be unstable in high-dimensional settings particularly when  $n \ll d$ . Therefore,  $\hat{\Sigma}$  may become ill-conditioned or singular even under robust procedures. Second, their geometric structure remains inherently elliptical and the resulting contours may fail to accurately reflect the underlying data geometry. Consequently, although robust Mahalanobis distances mitigate the sensitivity of the classical approach, they remain fundamentally tied to covariance-based geometry.

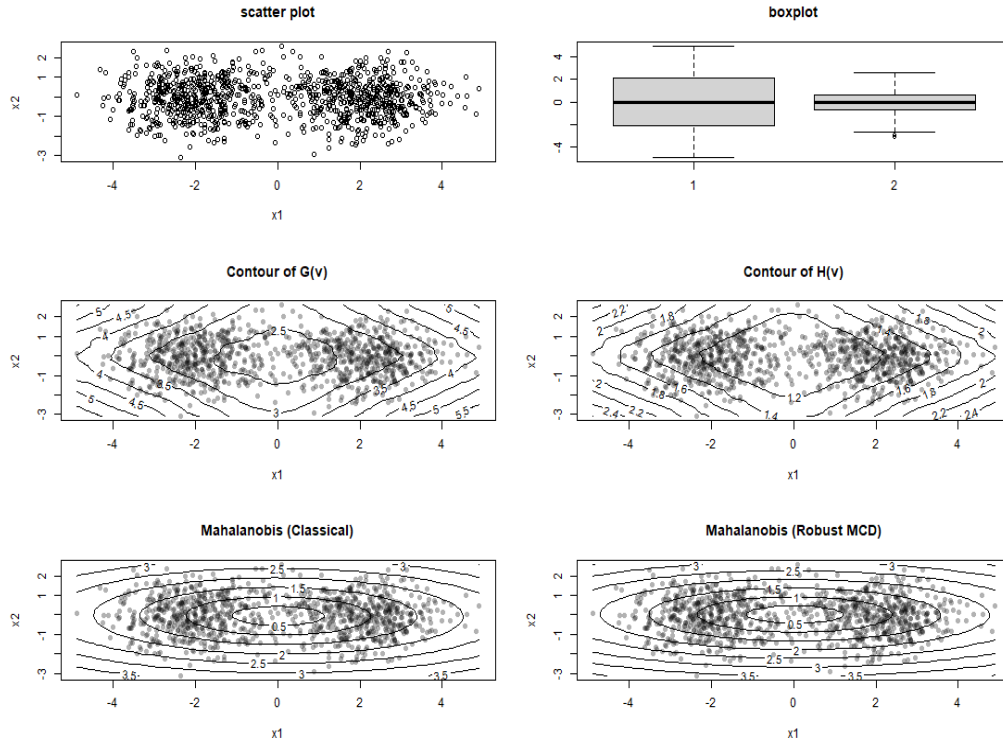


Fig 4. Comparison of median–radius contours and Mahalanobis distance under bimodal data

Figure 4 is generated as a two-component Gaussian mixture with  $n = 1000$  observations. The first component consists of  $n/2$  points sampled from a bivariate normal distribution with mean  $(-2,0)$  and covariance matrix equal to the identity, while the second component contains  $n/2$  observations from a similar distribution centred at  $(2,0)$ . This construction produces a horizontally separated bimodal distribution with relatively homogeneous variance in both directions. The scatter plot (top-left) clearly reveals two well-defined clusters along the  $x_1$ -axis, while the boxplots (top-right) highlight the larger spread and bimodality in  $x_1$  compared to the more concentrated and centered distribution of  $x_2$ .

The contour plots of the median–radius functional  $G(v)$  and its normalized version  $H(v)$  (middle row) exhibit non-elliptical, diamond-shaped regions that adapt to the bimodal structure, reflecting the balance between distances to the two clusters. This figure clearly demonstrates that the normalized median–radius functional  $H(v)$  captures the true geometry of the data, including bimodality and asymmetry, whereas both classical and robust Mahalanobis distances impose an elliptical structure that fails to reflect these features.

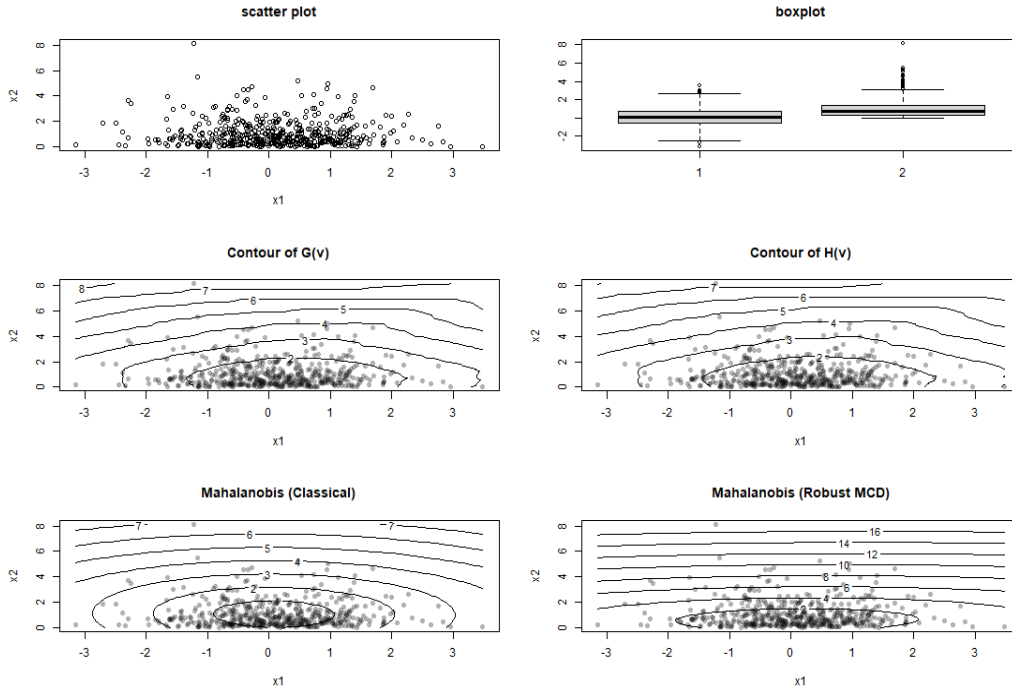


Figure 5. Comparison of median-radius contours and Mahalanobis distance under Asymmetric data

The skewed dataset is generated by combining a symmetric normal variable with an exponentially distributed variable, producing a bi-marginal distribution that is symmetric in one direction and strongly skewed in the other. This design allows clear assessment of how different methods capture directional asymmetry.

Figure 5 illustrates that the normalized median-radius functional  $H(v)$  provides a robust, geometry-driven representation of centrality that adapts to skewness and tail behaviour. In contrast, classical and robust Mahalanobis distances cannot capture the intrinsic asymmetry of the data where they impose symmetric elliptical structure..

Figure 6 shows the high-dimensional setting where the number of variables exceeds the number of observations ( $d > n$ ). The sample covariance matrix becomes singular and rendering the classical Mahalanobis distance undefined. On the other hand, the median-radius functional  $G(v)$  depends only on pairwise Euclidean distances. It remains well-defined and computationally stable. The resulting contours of  $G(v)$  and its normalized version  $H(v)$  preserve a coherent geometric structure, demonstrating robustness and applicability in high-dimensional regimes where covariance-based methods fail.

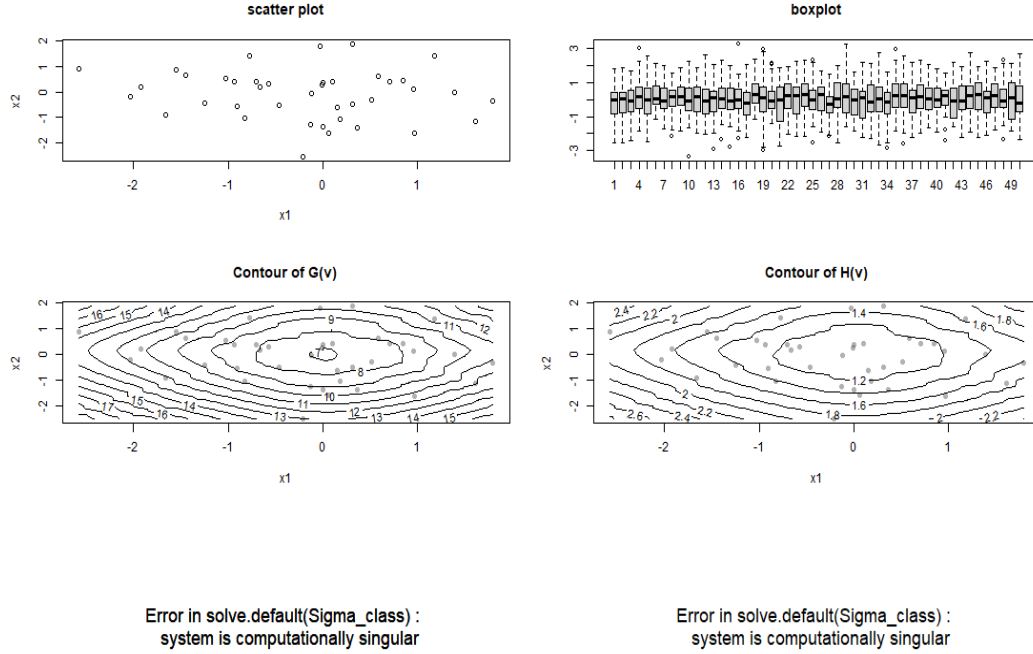


Figure 6. behaviour of  $G(v)$  and  $H(v)$  in high dimensions compared to the breakdown of Mahalanobis distance ( $d > n$ ).

### 4.3 Depth measure

Statistical depth functions provide a principled framework for ordering multivariate observations according to their centrality relative to a distribution. We introduce a novel depth measure derived from the median–radius functional through the normalized quantity  $H(v)$ . All computations depend on R-software (R Core Team, 2026) and depth packages (Kosiorowski D., 2019; Nordhausen, 2018; Pokotylo et al., 2019).

#### Theorem 2 (Median–Radius Depth)

Let  $X \in \mathbb{R}^d$  be a random vector with distribution  $P$ , and define the median–radius functional

$$G(v) := \inf \left\{ r \geq 0 : P(\|X - v\| \leq r) \geq \frac{1}{2} \right\}.$$

Let  $M \in \arg \min_{v \in \mathbb{R}^d} G(v)$ , and define the depth function

$$D_{MRD}(v) := \frac{1}{H(v)} = \frac{G(m)}{G(v)} = \frac{\text{minimal 50\% radius}}{\text{radius at } v}$$

Then  $D_{MRD}(v)$  is a valid statistical depth function in the sense of Zuo and Serfling (2000), satisfying maximality at the center, monotonicity relative to the center, vanishing at infinity, and convex, nested central regions.

*Proof.* See Appendix.

The depth  $D_{MRD}(v)$  admits a natural geometric interpretation where deep points correspond to locations that achieve efficient coverage of the data (small median radius), whereas shallow points require larger radii to capture half of the probability mass. A key advantage of the

proposed depth is its sensitivity to the geometry of the data. Because  $G(v)$  is defined through median distances, the resulting depth is inherently robust to extreme observations. In contrast to covariance-based methods, the level sets of  $H(v)$  and  $D_{\text{MRD}}(v)$  are not restricted to elliptical shapes. Instead, they adapt flexibly to the structure of the data to capture skewness, tail behaviour, multimodality, and cluster separation. Under elliptical symmetry,  $D_{\text{MRD}}(v)$  reduces to a monotone transformation of Mahalanobis depth. However, for skewed or multimodal distributions, it provides a strictly richer and more geometrically faithful representation of centrality.

#### 4.4 Comparison with classical depth functions

This section presents simulation studies and graphical illustrations to evaluate the behaviour of the proposed median–radius depth  $D_{\text{MRD}}(v)$  and to compare it with several classical depth measures. The following depth functions are considered,

The projection depth

$$D_{\text{proj}}(v; F) = \left( 1 + \sup_{u \in \mathbb{S}^{d-1}} \frac{|u^T v - \text{Med}(u^T X)|}{\text{MAD}(u^T X)} \right)^{-1},$$

which evaluates the worst standardized deviation over all projection directions. It is explicitly extremal and sensitive to directional outliers (Mosler & Mozharovskyi, 2022; Zuo, 2003).

Spatial depth

$$D_{\text{sp}}(v; F) = 1 - \left\| \mathbb{E} \left[ \frac{X - v}{\|X - v\|} \right] \right\|,$$

which averages directional information through spatial signs, providing a smooth and moment-free notion of centrality (Serfling & Wijesuriya, 2017; Zuo & Serfling, 2000).

Tukey (halfspace) depth

$$D_{\text{Tukey}}(v; F) = \inf_{u \in \mathbb{S}^{d-1}} \mathbb{P}(u^T X \leq u^T v),$$

which measures the minimum probability mass contained in any halfspace including  $v$ . It provides a strong geometric notion of centrality based on data depth regions (Nagy, 2025; Tukey, 1975). The Simplicial depth

$$D_{\text{simp}}(v; F) = \mathbb{P}(v \in \text{conv}(X_1, \dots, X_{d+1})),$$

where  $X_1, \dots, X_{d+1}$  are independent copies of  $X$ . This measures the probability that  $v$  lies inside a random simplex and represents a purely combinatorial notion of centrality (Liu, 1990).

The Mahalanobis depth

$$D_M(v) = \frac{1}{1 + (v - \mu)^T \Sigma^{-1} (v - \mu)},$$

which is based on the covariance structure and induces elliptical contours (“Reprint of: Mahalanobis, P.C. (1936) ‘On the Generalised Distance in Statistics.’” 2018).

The proposed median–radius depth

$$D_{\text{MRD}}(v) = \frac{G(M)}{G(v)},$$

differs fundamentally from classical depth notions in several respects:

- Covariance independence:  $D_{\text{MRD}}(v)$  does not rely on moment assumptions or covariance estimation and therefore remains well-defined in heavy-tailed and high-dimensional settings.

- Radial vs directional formulation: Tukey and projection depths are based on directional projections and halfspaces.  $D_{MRD}(v)$  relies on radial coverage via Euclidean balls that providing a complementary geometric perspective.
- Median-based robustness: while spatial depth depends on expectations of directional vectors.  $D_{MRD}(v)$  is based on median distances and protect robustness against outliers.
- Computational simplicity: in contrast to simplicial depth, which involves combinatorial complexity.  $D_{MRD}(v)$  is straightforward to compute via distance-based quantities.

For empirical comparison, we employ rank correlation to assess global agreement between depth functions and depth-weighted centre. A centre estimate is computed as a depth-weighted average

$$\hat{c} = \frac{\sum_{i=1}^n D(X_i) X_i}{\sum_{i=1}^n D(X_i)}.$$

This provides a quantitative measure of how each method defines the “centre” of the data. Differences between these centres reflect variations in the underlying notion of centrality. The simulation design generates bivariate observations  $X = (X_1, X_2)$  under three distributional settings. In the Gaussian case, the data are generated as

$$X \sim N_2 \left( \begin{bmatrix} 0 \\ 0 \end{bmatrix}, I_2 \right),$$

so both components are independent. Standard normal variables produce a symmetric unimodal elliptical cloud. In the skewed case, the first component remains normal while the second component follows a shifted exponential distribution,

$$X_1 \sim N(0,1), X_2 \sim \text{Exp}(1) - 1,$$

which creates a non-elliptical distribution with positive skewness in the second direction and approximately centred mean. In the multimodal case, the data are generated from a two-component Gaussian mixture,

$$X \sim \frac{1}{2} N_2 \left( \begin{bmatrix} -2 \\ 0 \end{bmatrix}, I_2 \right) + \frac{1}{2} N_2 \left( \begin{bmatrix} 2 \\ 0 \end{bmatrix}, I_2 \right),$$

producing two separated clusters and a bimodal structure. Thus, the simulation moves from an ideal symmetric Gaussian setting to a skewed non-normal setting.

Table 1. correlation and estimated centre measure  $\hat{c}$  for depth measures using Guassain data

	H ( $D_{RMD}$ )	Mahalanobis	Tukey	Spatial	Simplicial	Projection
			Corr.			
H ( $D_{RMD}$ )	1.000	0.998	0.997	0.998	0.997	0.999
Mahalanobis	0.998	1.000	0.999	1.000	0.999	1.000
Tukey	0.997	0.999	1.000	1.000	1.000	0.998
Spatial	0.998	1.000	1.000	1.000	1.000	0.999
Simplicial	0.997	0.999	1.000	1.000	1.000	0.999
Projection	0.999	1.000	0.998	0.999	0.999	1.000
			centre			
H ( $D_{RMD}$ )	0.000	0.002	0.005	0.003	0.005	0.002
Mahalanobis	0.002	0.000	0.003	0.002	0.002	0.000
Tukey	0.004	0.003	0.000	0.003	0.002	0.003
Spatial	0.003	0.002	0.003	0.000	0.004	0.001
Simplicial	0.005	0.002	0.002	0.004	0.000	0.002
Projection	0.002	0.000	0.003	0.001	0.002	0.000

Table 1 summarizes the results obtained from 3,000 simulation trials based on a bivariate normal distribution with diagonal covariances. All depth functions considered exhibit perfect agreement, with rank correlation equal to one across all methods. In addition, the estimated centres coincide, with negligible numerical differences.

This confirms that the proposed median–radius depth is consistent with classical depth notions under elliptical symmetry, where different depth functions are known to be equivalent up to monotone transformations. These results validate both the correctness of the implementation and the theoretical property that the proposed method does not deviate from classical approaches in symmetric settings.

Table 2. correlation and estimated centre measure  $\hat{c}$  for depth measure using skewed data

	H ( $D_{RMD}$ )	Mahalanobis	Tukey	Spatial	Simplicial	Projection
			Corr.			
H ( $D_{RMD}$ )	1.000	0.947	0.851	0.953	0.831	0.989
Mahalanobis	0.947	1.000	0.930	0.991	0.911	0.916
Tukey	0.851	0.930	1.000	0.957	0.993	0.832
Spatial	0.953	0.991	0.957	1.000	0.942	0.925
Simplicial	0.841	0.911	0.993	0.942	1.000	0.814
Projection	0.989	0.916	0.832	0.925	0.814	1.000
			center			
H ( $D_{RMD}$ )	0.000	0.004	0.027	0.005	0.017	0.038
Mahalanobis	0.004	0.000	0.031	0.001	0.021	0.034
Tukey	0.027	0.031	0.000	0.032	0.011	0.065
Spatial	0.005	0.001	0.032	0.000	0.021	0.033
Simplicial	0.017	0.021	0.011	0.021	0.000	0.055
<b>Projection</b>	<b>0.038</b>	<b>0.034</b>	<b>0.065</b>	<b>0.033</b>	<b>0.055</b>	<b>0.000</b>

Table 2 illustrates the results obtained using 3,000 simulation trials from a skewed distribution (normal and exponential distributions). While rank correlations remain high overall, some differences emerge between methods. The proposed  $D_{MRD}(v)$  exhibits strong agreement with spatial and projection depth (correlations exceeding 0.95). It indicates that these methods share a common radial characterization of centrality. However, the correlation with Tukey and simplicial depth drops to approximately 0.85. It reflects differences in how these methods respond to asymmetry and tail behaviour.

Table 3. correlation and estimated centre measure  $\hat{c}$  for depth measures using multimodal data

	H ( $D_{RMD}$ )	Mahalanobis	Tukey	Spatial	Simplicial	Projection
			r			
H ( $D_{RMD}$ )	1.000	0.952	0.962	0.962	0.972	0.890
Mahalanobis	0.952	1.000	0.993	0.998	0.988	0.981
Tukey	0.962	0.993	1.000	0.997	0.995	0.971
Spatial	0.962	0.998	0.997	1.000	0.994	0.975
Simplicial	0.972	0.988	0.995	0.994	1.000	0.951
Projection	0.890	0.981	0.971	0.975	0.951	1.000
		centre	cent			
H ( $D_{RMD}$ )	0.000	0.010	0.012	0.008	0.005	0.019
Mahalanobis	0.010	0.000	0.003	0.002	0.005	0.009
Tukey	0.012	0.003	0.000	0.005	0.007	0.007
Spatial	0.008	0.002	0.005	0.000	0.003	0.011

Simplicial	0.005	0.005	0.007	0.003	0.000	0.014
Projection	0.019	0.009	0.007	0.011	0.014	0.000

Table 3 summarizes the results obtained from 3,000 simulation trials based on a bimodal normal distribution with component means at  $(-2, 0)$  and  $(2, 0)$ , each having diagonal covariance structure. The agreement between depth functions remains high, with rank correlations exceeding 0.95 for most method pairs.

Unlike the skewed case, the centre estimates remain nearly identical across all methods. This reflects the overall symmetry of the mixture distribution. Nevertheless, subtle differences emerge in the rankings especially between  $D_{MRD}(v)$  and projection depth where the correlation drops to about 0.90. This indicates that the proposed method captures aspects of the underlying cluster structure that are not fully represented by projection-based approaches.

Overall, the results suggest that while multimodality does not strongly affect central location estimates, it influences the ordering of points. Therefore, the proposed depth function is sensitive to these structural features.

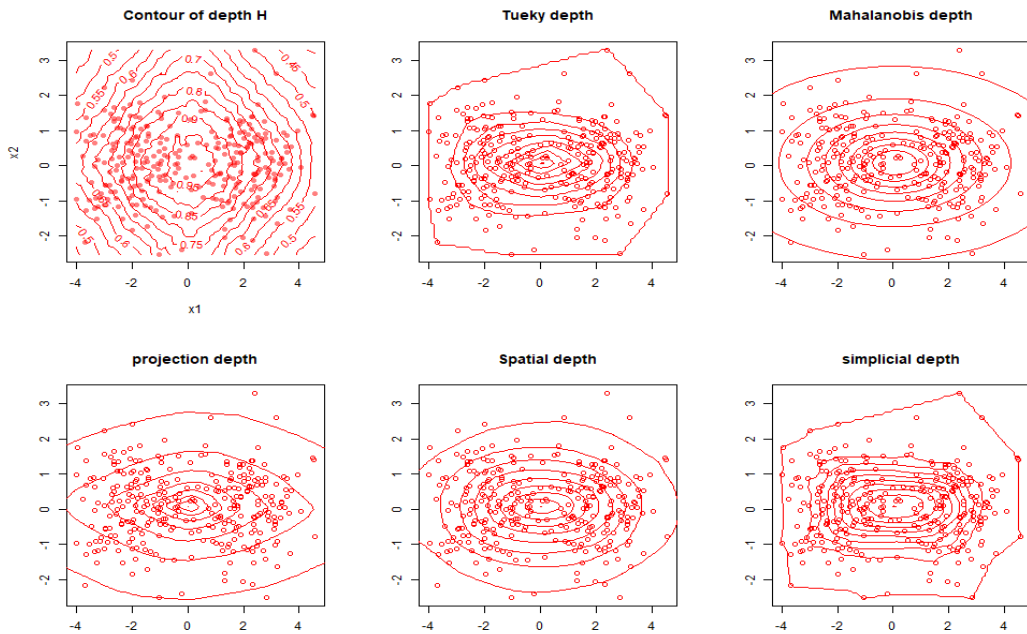


Figure 7. depth measures using different approaches of bimodal normal data.

Figure 7 illustrates contour plots for different depth functions of a bimodal dataset with two clusters centred at  $(-2, 0)$  and  $(2, 0)$ . The proposed median–radius depth  $D_{MRD}(v)$  produces non-elliptical contours that adapt to the underlying data geometry. In contrast the classical depth functions including Mahalanobis, spatial, Tukey, projection, and simplicial depth tend to impose symmetric or globally convex structures. This highlights the ability of the median–radius approach to capture complex features such as multimodality that are not fully represented by traditional depth measures.

## 5 Conclusion

This study introduces median–radius perspective for measuring centrality that departs from covariance-based and projection-based methodologies. Its importance lies in providing a

robust, covariance-free, and geometry-driven framework that remains valid under minimal assumptions. Unlike classical methods that impose elliptical or directional constraints, it adapts naturally to the intrinsic shape of the data, capturing multimodality, asymmetry, and local structure. We establish fundamental properties of  $G(v)$  including convexity and well-defined subgradient structure and show that its minimizers coincide with the medians of the distribution. The geometric interpretation of  $G(v)$  and its subgradients provides additional insight and revealing how directional imbalance in the data is captured through radial structure. The associated normalized function  $H(v)$  provides a scale-invariant measure of radial dispersion while its inverse defines a valid depth function  $D_{\text{MRD}}(v)$ . Unlike classical distance and depth methods, the proposed approach is covariance-free, relying solely on Euclidean distances. As a result, it is inherently robust, distribution-agnostic and remains stable in high-dimensional settings.

Through simulation study, we demonstrate that the proposed depth is consistent with classical methods under symmetry while offering a richer and more adaptive representation in the presence of skewness, multimodality, and contamination. In particular, the level sets of  $H(v)$  naturally reflect the intrinsic shape of the data and avoid the restrictive elliptical geometry imposed by covariance-based approaches.

Despite robustness and geometric appeal of  $G(v)$  and  $H(v)$ , they may overlook small-scale structures and be less efficient under ideal parametric conditions.

## References

- Boente, G., & Salibián-Barrera, M. (2021). Robust functional principal components for sparse longitudinal data. *METRON*, 79(2), 159–188. <https://doi.org/10.1007/s40300-020-00193-3>
- Boyd, S., & Vandenberghe, L. (2004). *Convex Optimization*. Cambridge University Press. <https://doi.org/10.1017/CBO9780511804441>
- Capezza, C., Centofanti, F., Lepore, A., & Palumbo, B. (2024). Robust Multivariate Functional Control Chart. *Technometrics*, 66(4), 531–547. <https://doi.org/10.1080/00401706.2024.2327346>
- Chaudhuri, P. (1996). On a Geometric Notion of Quantiles for Multivariate Data. *Journal of the American Statistical Association*, 91(434), 862–872. <https://doi.org/10.1080/01621459.1996.10476954>
- Deb, N., & Sen, B. (2023). Multivariate Rank-Based Distribution-Free Nonparametric Testing Using Measure Transportation. *Journal of the American Statistical Association*, 118(541), 192–207. <https://doi.org/10.1080/01621459.2021.1923508>
- Elamir, E. (2025). Data Analytics and Distribution Function Estimation via Mean Absolute Deviation: Nonparametric Approach. *REVSTAT – Statistical Journal*, 23(1), 79–100.
- Hubbard, J. H. , & H. B. B. (2015). *Vector calculus, linear algebra, and differential forms: a unified approach* . Matrix Editions.
- Hubert, M., Rousseeuw, P. J., & Vanden Branden, K. (2005). ROBPCA: A New Approach to Robust Principal Component Analysis. *Technometrics*, 47(1), 64–79. <https://doi.org/10.1198/004017004000000563>

- Johnson R., & Wichern D. (2002). *Applied multivariate statistical analysis*. John Wiley & Sons.
- Kosiorowski D., Z. Z. (2019). DepthProc: An R Package for Robust Exploration of Multidimensional Economic Phenomena. *ArXiv Preprint ArXiv:1408.4542*.
- Lange, T., Mosler, K., & Mozharovskyi, P. (2014). Fast nonparametric classification based on data depth. *Statistical Papers*, 55(1), 49–69. <https://doi.org/10.1007/s00362-012-0488-4>
- Lin, L., & Chen, M. (2006). Robust estimating equation based on statistical depth. *Statistical Papers*, 47(2), 263–278. <https://doi.org/10.1007/s00362-005-0287-2>
- Liu, R. Y. (1990). On a Notion of Data Depth Based on Random Simplices. *The Annals of Statistics*, 18(1), 405–414.
- Mosler, K., & Mozharovskyi, P. (2022). Choosing Among Notions of Multivariate Depth Statistics. *Statistical Science*, 37(3). <https://doi.org/10.1214/21-STS827>
- Nagy, S. (2025). Halfspace Depth. *WIREs Computational Statistics*, 17(3). <https://doi.org/10.1002/wics.70038>
- Nordhausen, K. , S. S. , O. H. , T. D. E. , & N. M. K. (2018). Package ‘ICSNP’. *Tampere University*.
- Pawar, S. D., & Shirke, D. T. (2022). Data Depth-Based Nonparametric Tests for Multivariate Scales. *Journal of Statistical Theory and Practice*, 16(1), 11. <https://doi.org/10.1007/s42519-021-00236-6>
- Pokotylo, O., Mozharovskyi, P., & Dyckerhoff, R. (2019). Depth and Depth-Based Classification with R Package **ddalpha**. *Journal of Statistical Software*, 91(5). <https://doi.org/10.18637/jss.v091.i05>
- R Core Team. (2026). *R: A Language and Environment for Statistical Computing*. <https://www.R-project.org/>.
- Reprint of: Mahalanobis, P.C. (1936) “On the Generalised Distance in Statistics.” (2018). *Sankhya A*, 80(S1), 1–7. <https://doi.org/10.1007/s13171-019-00164-5>
- Rousseeuw, P. J., & Croux, C. (1993). Alternatives to the Median Absolute Deviation. *Journal of the American Statistical Association*, 88(424), 1273–1283. <https://doi.org/10.1080/01621459.1993.10476408>
- Rousseeuw, P. J., & Driessen, K. Van. (1999). A Fast Algorithm for the Minimum Covariance Determinant Estimator. *Technometrics*, 41(3), 212–223. <https://doi.org/10.1080/00401706.1999.10485670>
- Serfling, R., & Wijesuriya, U. (2017). Depth-based nonparametric description of functional data, with emphasis on use of spatial depth. *Computational Statistics & Data Analysis*, 105, 24–45. <https://doi.org/10.1016/j.csda.2016.07.007>
- Tukey, W. J. (1975). Mathematics and the Picturing of Data. *Proceedings of the International Congress of Mathematicians*, 523–531.

Zuo, Y. (2003). Projection-Based Depth Functions and Associated Medians. *Annals of Statistics*, 31(5), 1460–1490.

Zuo, Y., & Serfling, R. (2000). General Notions of Statistical Depth Function. *The Annals of Statistics* ., 28(2), 461–482.

## Appendix

### Proof of theorem 1.

From definition 1

$$S(v, t) = \mathbb{P}(|X - v| \leq t) = F(v + t) - F(v - t),$$

the function  $G(v)$  is characterized by

$$S(v, G(v)) = \frac{1}{2},$$

with  $G(v)$  minimal. Since  $F$  is continuous,  $S(v, t)$  is continuous and strictly increasing in  $t$ , which ensures uniqueness of  $G(v)$ .

Fix  $v \in \mathbb{R}$ , and let  $h$  be small. For  $v + h$ , the defining equation becomes

$$F(v + h + G(v + h)) - F(v + h - G(v + h)) = \frac{1}{2}.$$

Subtract from  $F(v + G(v)) - F(v - G(v)) = \frac{1}{2}$ .

Because  $F$  is continuous (and monotone), we may write the difference as

$$0 = [F(v + h + G(v + h)) - F(v + G(v))] - [F(v + h - G(v + h)) - F(v - G(v))].$$

Divide by  $h$ , and consider the limit as  $h \rightarrow 0$  from the left or the right. Since  $G$  is convex, the one-sided limits exist. As  $h \rightarrow 0$ ,

$$\frac{G(v + h) - G(v)}{h} \rightarrow G'_-(v) \text{ or } G'_+(v),$$

depending on the direction. Using monotonicity of  $F$ , passage to the limit yields

$$0 = \mathbb{P}(X \leq v - G(v)) - \mathbb{P}(X \geq v + G(v)) + G'(v),$$

where  $G'(v)$  is interpreted as the appropriate one-sided derivative. Rearranging gives the stated expressions.

Moreover, where each probability term lies in  $[0,1]$ , hence

$$G'_-(v), G'_+(v) \in [-1,1].$$

Since  $G$  is convex, it must satisfy  $G'_-(v) \leq G'_+(v)$ , by definition,  $v$  is a median of  $X$  if and only if

$$\mathbb{P}(X \leq v) \geq \frac{1}{2} \text{ and } \mathbb{P}(X \geq v) \geq \frac{1}{2}.$$

Using  $S(v, G(v)) = \frac{1}{2}$ , this is equivalent to

$$\mathbb{P}(X \leq v - G(v)) \leq \frac{1}{2} \quad \text{and} \quad \mathbb{P}(X \geq v + G(v)) \leq \frac{1}{2},$$

which in turn is equivalent to

$$0 \in [G'_-(v), G'_+(v)].$$

This completes the proof.

**Proof of collar 1.**

From Theorem 1,

$$\begin{aligned} G'_+(v) - G'_-(v) &= [\mathbb{P}(X \geq v - G(v)) - \mathbb{P}(X < v + G(v))] \\ &\quad - [\mathbb{P}(X \leq v - G(v)) - \mathbb{P}(X > v + G(v))]. \end{aligned}$$

Rearranging terms yields

$$G'_+(v) - G'_-(v) = [\mathbb{P}(X = v - G(v))] + [\mathbb{P}(X = v + G(v))],$$

which proves the stated formula.

**Proof theorem 2.**

- Maximality at the center: By definition of  $m$ ,  $G(m) \leq G(v), \forall v \in \mathbb{R}^d$ . Thus,

$$D_{MRD}(v) = \frac{G(m)}{G(v)} \leq 1,$$

with equality if and only if  $v = m$  (when the minimizer is unique),  $D_{MRD}(m) = 1 = \sup_v D(v)$ . So the maximum depth occurs at the centre.

- Monotonicity relative to the centre: Fix a direction  $u \in \mathbb{S}^{d-1}$ , and define  $v(t) = m + tu, t \geq 0$ . Moving away from  $m$  shifts the centre of the ball away from the bulk of the distribution, so a larger radius is required to cover at least 50% probability. Thus,

$$t_1 < t_2 \implies G(v(t_1)) \leq G(v(t_2)).$$

Hence,

$$D(v(t)) = \frac{G(m)}{G(v(t))}$$

is nonincreasing in  $t$ . Depth decreases as we move away from the centre.

- Vanishing at infinity: Let  $\|v\| \rightarrow \infty$ . Then for any fixed  $X$ ,  $\|X - v\| \geq \|v\| - \|X\|$ . Thus,  $\|X - v\| \rightarrow \infty$  in probability, implying  $G(v) \rightarrow \infty$ . Therefore,  $D(v) = \frac{G(m)}{G(v)} \rightarrow 0$  and  $\lim_{\|v\| \rightarrow \infty} D(v) = 0$ .
- Convexity and nestedness of central regions: The depth regions are given by:

$$\{v: D(v) \geq \alpha\} = \left\{v: G(v) \leq \frac{G(m)}{\alpha}\right\}.$$

Since:  $v \mapsto \|X - v\|$  is convex, the median operator preserves convexity under mild regularity conditions, we have  $G(v)$  is convex. Hence, the sublevel sets:  $\{v: G(v) \leq c\}$  are convex. Nestedness follows immediately

$$\alpha_1 \leq \alpha_2 \implies \{D(v) \geq \alpha_2\} \subset \{D(v) \geq \alpha_1\}.$$

All defining properties of a statistical depth function are satisfied.